Attraction and repulsion of spiral waves by localized inhomogeneities in excitable media

Alberto P. Muñuzuri,* Vicente Pérez-Muñuzuri, and Vicente Pérez-Villar

Nonlinear Physics Group, Faculty of Physics, University of Santiago de Compostela, 15706 Santiago de Compostela, Spain

(Received 16 January 1998; revised manuscript received 17 April 1998)

The anchoring and repelling of spiral waves in a two-dimensional homogeneous excitable medium in the presence of a localized defect is studied in the framework of a numerical model and the kinematical theory. Depending on the relative initial distance between the obstacle and the core center, the vortex is observed either to drift towards the obstacle or to move away from it. The anchoring phenomenon is explained in terms of periodic perturbations of the front curvature, while the repulsion is rather connected with inhomogeneous refractoriness, which affects the spiral tip motion.
[S1063-651X(98)51509-7]

PACS number(s): 82.40.Ck, 03.40.Kf, 47.54.+r, 87.45.Bp

[1]Experimental observations of vortices in excitable media have demonstrated the significant effect of heterogeneities on the motion of vortex waves. These effects include the drift of vortices due to parameter gradients [1–3] or external influences [4–7], and the anchoring of vortices on localized inhomogeneities or defects [1,3]. These phenomena have been observed in autocatalytic reactions as well as in the myocardial tissue. In the latter case, drift and anchoring of vortices are thought to underlie pathological situations in which high frequency rhythms persist and can lead to fibrillation of the heart [1,3]. Thus, localized inhomogeneities (with a length scale comparable to or smaller than the wavelength) can lead to *pinning* or *anchoring* of the vortex [8–11].

Vinson *et al.* [12] observed the anchoring of three-dimensional (3D) vortices in inhomogeneous media and compared their results to previous ones in 2D media. They noticed that, depending on the distance between the drifting tip of the vortex and the defect, the spiral wave will either anchor to the defect or pass it. The situation becomes more complex as 3D vortices are involved, since anchoring and subsequent detachment of the vortices can take place. Here, scroll waves naturally drifted, in the absence of a localized defect, since a smooth gradient perpendicular to the initial filament was imposed.

On the other hand, mechanisms to unpin a vortex in a 2D medium have been recently studied [13]. A vortex can be unpinned when a new created vortex is pinned to the same obstacle and has any topological charge. Similar mechanisms may underlie antitachycardia pacing used in cardiac clinics [14].

In this Rapid Communication we study, both numerically and theoretically, the influence of obstacles on the spiral wave dynamics in a two-dimensional homogeneous medium. In the absence of localized defects, the spiral wave remains steadily rotating around a circular core. In contrast, we observed that depending on the initial distance between a localized inhomogeneity and the spiral tip position, vortices can be attracted or repelled by the defect. In the first case, the spiral, after drifting towards the obstacle, is anchored there.

*Electronic address: uscfmapm@cesga.es

Numerical experiments have been performed with a two-variable Oregonator model modified to describe the effect of light on the medium [15,16],

$$\frac{\partial u}{\partial t}=\frac{1}{\varepsilon}\left(u-u^2-(fv+\phi)\frac{u-q}{u+q}\right)+D_u\nabla^2 u,$$
$$\frac{\partial v}{\partial t}=(u-v)+D_v\nabla^2 v, \tag{1}$$

where u and v describe the activator and the inhibitor variables, respectively ($HBrO_2$ and catalyst concentrations, respectively). D_u and D_v are the diffusion coefficients of both variables. f, q, and ε are parameters that are related to the kinetics of the Belousov-Zhabotinsky reaction. ϕ represents the light-induced flow of Br^-. Zero-flux boundary conditions were considered for u and v at the boundaries.

Obstacles in the medium were simulated by homogeneously illuminating the medium with $\phi=0$ except for a circular region (of radius 0.7 s.u.), with $\phi=0.11$. This value is enough to inhibit wave propagation along this small region. The radius of the obstacle was set slightly smaller than that of a free spiral core (≈ 0.9 s.u.) and was always placed such that the trajectory of the free tip (which is circular when it is free of any external perturbation and $\phi=0$) never enters in this region.

With this setup we studied different initial distances d between the center of a fully developed spiral wave core and the center of the obstacle, and we observed its evolution. Figure 1 shows typical evolutions of the core center observed in such a system for different initial values of d. For small values of d, the spiral is attracted to the obstacle and slowly approaches it until it anchors there. For values of d larger than 3.5 s.u. the spiral drifts away, far from the obstacle until it reaches $d\approx 7.5$ s.u. where the drift velocity becomes zero.

Figure 2 shows the variation of the spiral velocity (in polar coordinates, V_{rad}) as a function of d. The polar coordinates considered here are such that the center of coordinates is the obstacle center and the 0° angle is given by the positive direction of the OX axis. Here again, the two characteristic behaviors are clearly seen: for $d<3.5$ s.u., attraction occurs ($V_{rad}<0$), while for $d>3.5$ s.u., the spiral is

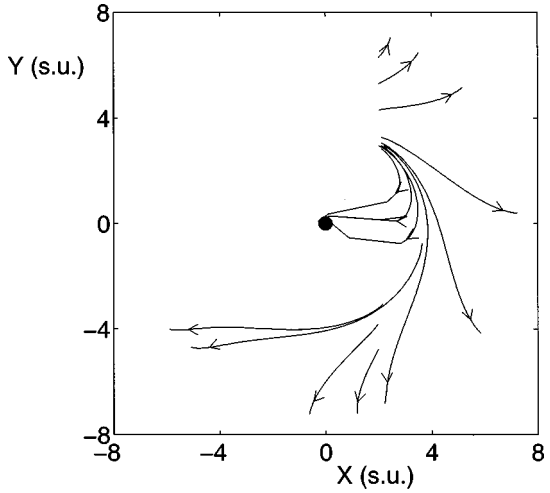

FIG. 1. Trajectory followed by the spiral core center starting at different initial distances from the obstacle. The obstacle is represented here as a black dot in the center of the image. Note that, for short distances, the spiral is attracted to the obstacle, while it is repelled for larger ones. Parameters for the Oregonator model [Eq. (1)] are: $f=1.4$, $q=0.002$, $\varepsilon=0.05$, $D_u=1$, and $D_v=0.6$. Spiral rotation period: 3.2 t.u.; wavelength: $\lambda=12$ s.u. t.u. and s.u. are the dimensionless time and space units, respectively, from Eq. (1).

repelled ($V_{rad}>0$). For the particular value of $d=3.5$ s.u., the spiral does not drift at all. Notice the presence of a minimum and a maximum in the radial velocity values for $d \approx 1.7$ and $d \approx 4.5$ s.u. For $d>8$ s.u., the spiral stops to drift away from the obstacle. The reason is that, at this point, the obstacle starts perturbing the second wave of the spiral wave and the effect is decreased dramatically [17–19]. In principle, there should be a very small velocity but the spatial discretization scheme that is used prevents us from measuring it. In Fig. 2, the results of many experiments (each considering a different initial value of d) are plotted. Nevertheless, all of the measured velocities fit in the same curve, which stresses the independence of the phenomenon with respect to the initial configuration.

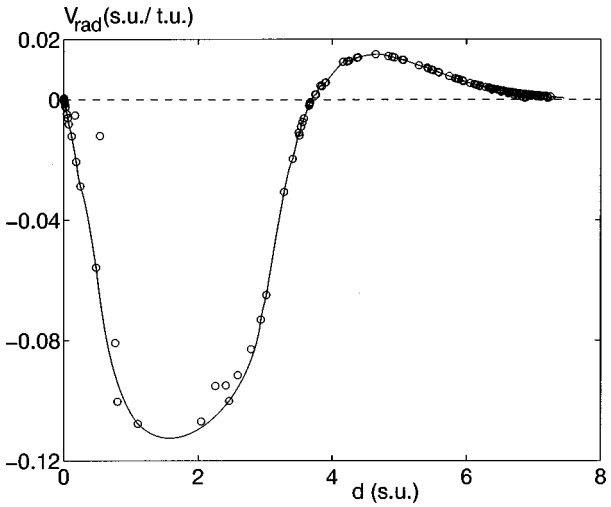

FIG. 2. Dependence of V_{rad} on the distance between the core and the obstacle centers, d, obtained with the Oregonator model [Eq. (1)]. The curve represents a fitting of the numerical data for better visualization. (Model parameters as in Fig. 1).

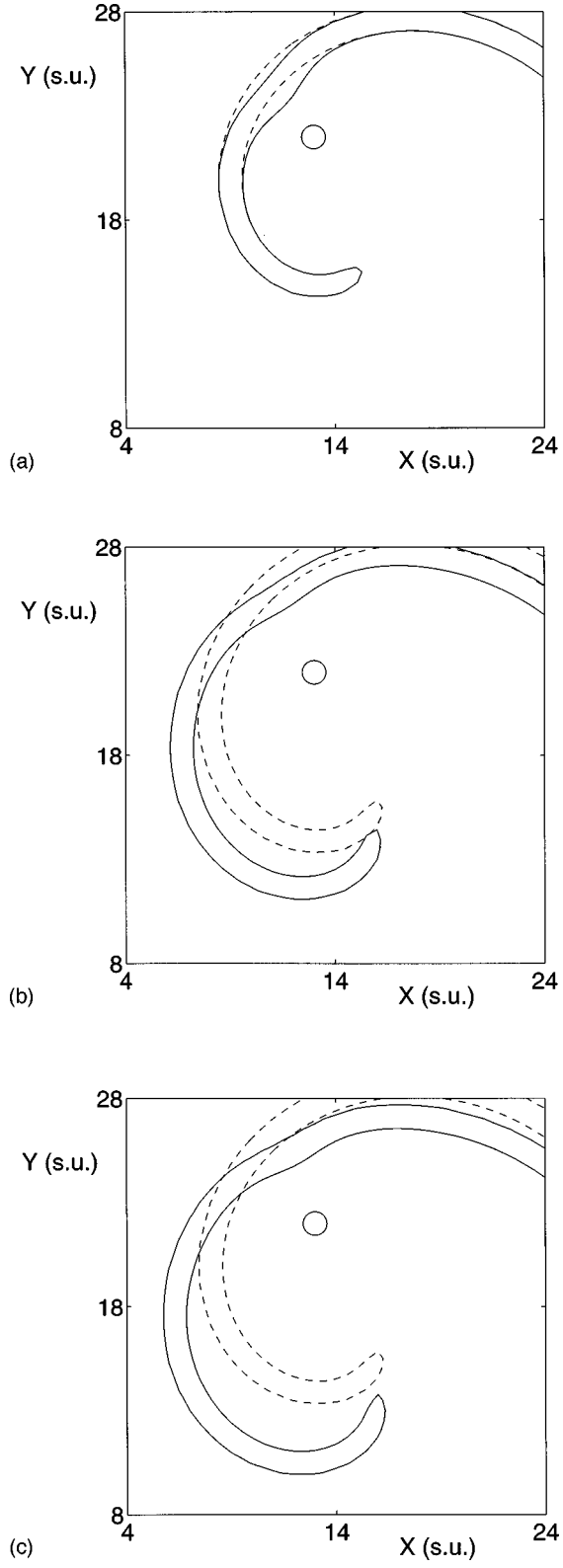

FIG. 3. Numerical evolution of a spiral wave (continuous line) separated from the obstacle by a distance $d=5.1$ s.u. in comparison to a free vortex (dashed line) moving in a homogeneous medium. Note the perturbation of the wave front after passing through the obstacle (represented here as a circle). (a)–(c) correspond to times 1.5, 218.5, and 770 t.u. Note the increasing separation among the free vortex and the controlled one while time goes on. (Model parameters as in Fig. 1).

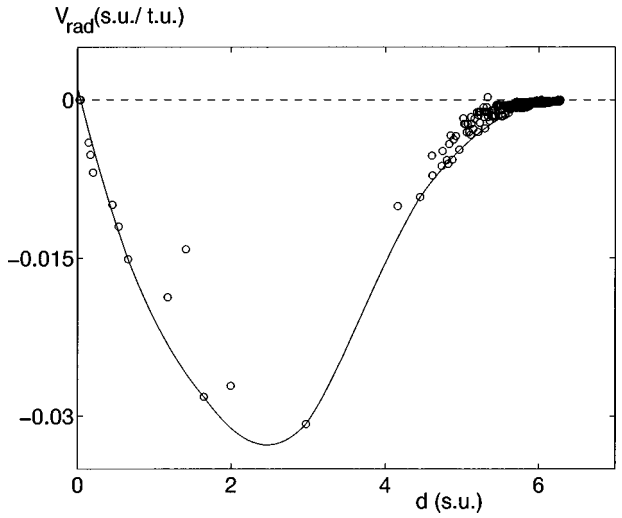

FIG. 4. Dependence of V_{rad} on the distance between the core and the obstacle centers, d, obtained with the kinematical model. The curve represents a fitting of the numerical data for better visualization. Set of parameters for the kinematical equations as in Ref. [21]: $V_0=1.5$, $\gamma=1.5$, $D=1.0$, and $G_0=1.2$; For Eq. (2): $\overline{k}=0.1$, $\xi=0.3$, and $\delta t=0.01$; core radius: 2.3 s.u.

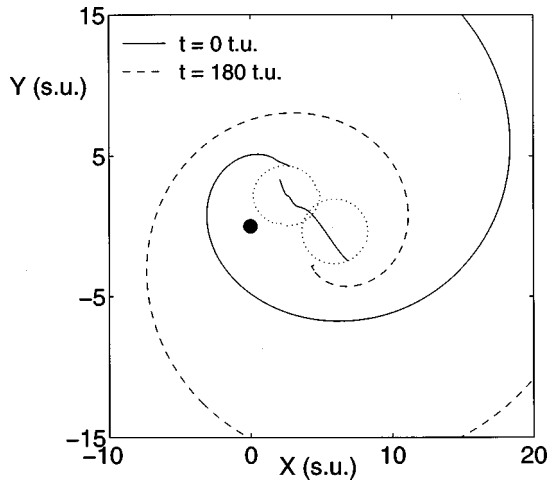

FIG. 5. Evolution of a spiral wave initially separated from the obstacle by a distance $d=3.7$ s.u. obtained with the kinematical model. The trajectory followed by the spiral core, when drifting away from the inhomogeneity (black dot), is shown as a continuous line. Dashed circles correspond to the initial and final trajectories of the tip. The spiral wave is shown at two different times: 0 (solid line) and 180 (dashed line) t.u. Parameters for Eq. (3): $\beta_v=\beta_g=5$ [20], and the remaining parameters as in Fig. 4.

Figure 3 shows the evolution of a vortex in the presence of an inhomogeneity in comparison with a free vortex rotating in a homogeneous medium. The initial distance d was such that the spiral wave drifts away from the obstacle. Note that the effect of the localized inhomogeneity slightly deforms the wave front as it goes through the obstacle. The effect of this bump (close to the tip where the distance between consecutive waves is smaller than the regular wavelength) is to cause the back of the first wave to approach the tip, thus partially inhibiting its propagation in this direction. The component of the tip velocity in that direction is then reduced so that it makes the spiral drift away from the obstacle.

The results shown in this Rapid Communication can be explained by the combination of two independent mechanisms. On the one hand, for small values of d ($d<3.5$ s.u.) the spiral is attracted to the obstacle and, consequently, moves in its direction until it anchors to that place. In order to explain these results qualitatively, we have solved the kinematical equations describing the motion of the spiral wave front [20,21], but we introduce the effect of a localized inhomogeneity as a small perturbation to the curvature

$$k(l,t+\delta t)=\begin{cases} k(l,t)-\overline{k}\exp(-l^2) & l\in[l_c-\xi,l_c+\xi] \\ k(l,t) \quad \text{otherwise,} \end{cases} \tag{2}$$

where $l_c=l_c(t)$ is the arc length measured from the free end of the curve to the center of the obstacle of radius ξ and $\overline{k}$ is the amplitude of the perturbation to the front curvature. l_c varies with time, its value decreasing as the spiral is attracted to the obstacle. The curvature of the front is periodically perturbed while the front crosses the obstacle located at a certain distance d from the initial position of the spiral tip. Figure 4 shows the relative tip velocity measured in polar coordinates as in Fig. 2. Note that only negative values of V_{rad} were obtained, since the spiral is only attracted to the obstacle. For large enough d, the spiral accelerates smoothly as it approaches the obstacle, until it reaches a maximum (in absolute value) for $d\approx 2.5$ s.u. and, from there on, it decelerates until it anchors to the obstacle ($V_{rad}=0$ and $d=0$). This behavior was observed in Fig. 2 as well. The actual mechanism responsible for this effect is determined by the motion of the bump towards the tip. When it reaches the free end, the main effect is to introduce a shift in the rotation angle of the tip. The shape of the spiral curve near its tip is recovered after the perturbation reaches the free end within a time that is much shorter than the rotation period of the spiral [21]. So when the front reaches the obstacle again, it has its initial shape but the tip is smoothly displaced from its original position. The accumulation of these shifts as the spiral keeps on rotating results in its global drift towards the obstacle.

On the other hand, for large values of d, the perturbation to the wave front moves away from the tip. Its effect on the wave propagation is not reflected in Fig. 4 since, for the kinematical model developed above, we assumed that the propagation velocity of an excitation wave depends only on the local curvature of its front. This implies that the back of the previous propagating wave front does not affect the next one. However, from Fig. 3 it is clear that this is the main mechanism responsible for the repulsion of the vortex by the localized inhomogeneity. To avoid this limitation, to some extent, it is necessary to include the effect of the refractoriness [20] in the kinematical equations. With this in mind, both the eikonal equation describing the front velocity in its normal direction, $V(l)$, and the sprouting tangent velocity at the tip of the spiral, G, have been modified as follows [20]:

$$\begin{aligned} V(l)&=V_0[1-\beta_v/T(x,y)]-Dk(l), \\ G&=G_0[1-\beta_g/T(x,y)]-\gamma k(0), \end{aligned} \tag{3}$$

where $T(x,y)$ accounts for the refractoriness of the wave front and is measured as the time interval from the moment of the last passage of an excitation wave through a given point with coordinates x and y. β_v and β_g are some positive coefficients. Now, after solving the set of kinematical equations given in Ref. [21] and Eqs. (2) and (3), the curve shown in Fig. 2 can be recovered. For values of d below some critical value, the spiral wave is attracted to the inhomogeneity, but for large enough d it is repelled. Figure 5 exemplifies the drift of a vortex away from the obstacle calculated with this kinematical model.

Traditionally, the existence of localized inhomogeneities in an excitable medium, such as cardiac tissue, has been associated with the attraction and subsequent anchoring of spiral waves (reentries), provided they are close enough to each other. Nevertheless, here we show the possibility of the opposite phenomenon where reentries can be repelled and eventually eliminated at the boundaries.

Our results suggest experiments on active media where the initial distance d, among the core center and the obstacle, can be precisely controlled, as well as a more detailed theoretical understanding based on a nonkinematical theory (as in Ref. [11]). Besides, these results are qualitatively different from those mentioned at the beginning of this Rapid Communication, since the drift of the spiral wave is *only* due to the presence of a localized inhomogeneity in the medium, and the vortex can be attracted to or repelled by the obstacle depending on the initial relative distance d.

This work was partially supported by the Comisión Interministerial de Ciencia y Tecnología under Project Nos. PB94-0623 and PB96-0937. The calculations were performed at the Supercomputation Center of Galicia (CESGA), Spain.

[1] J. M. Davidenko, A. M. Pertsov, R. Salomonz, W. Baxter, and J. Jalife, Nature (London) **335**, 349 (1992).

[2] V. G. Fast and A. M. Pertsov, J. Cardiovasc. Electrophysiol. **3**, 255 (1992).

[3] A. M. Pertsov, J. M. Davidenko, R. Salomonz, W. Baxter and J. Jalife, Circ. Res. **72**, 631 (1992).

[4] K. I. Agladze and P. DeKepper, J. Phys. Chem. **96**, 5239 (1992).

[5] O. Steinbock, J. Schütze, and S. C. Müller, Phys. Rev. Lett. **68**, 248 (1992).

[6] A. P. Muñuzuri, M. Gómez-Gesteira, V. Pérez-Muñuzuri, V. I. Krinsky, and V. Pérez-Villar, Phys. Rev. E **48**, 3232 (1993); **50**, 4258 (1994).

[7] A. P. Muñuzuri, C. Innocenti, J. M. Flesselles, J. M. Gilli, K. I. Agladze, and V. I. Krinsky, Phys. Rev. E **50**, 667 (1994).

[8] S. Nettesheim, A. von Oertzen, H. H. Rotermund, and G. Ertl, J. Chem. Phys. **98**, 9977 (1993).

[9] M. Bär, N. Gottschalk, M. Eiswirth, and G. Ertl, J. Chem. Phys. **100**, 1202 (1994).

[10] X. Zou, H. Levine, and D. A. Kessler, Phys. Rev. E **47**, 800 (1993).

[11] J. M. Starobin and C. F. Starmer, Phys. Rev. E **55**, 1193 (1997); **56**, 3757 (1997).

[12] M. Vinson, A. Pertsov, and J. Jalife, Physica D **72**, 119 (1994).

[13] V. I. Krinsky, F. Plaza, and V. Voignier, Phys. Rev. E **52**, 2458 (1995).

[14] M. E. Josephson, *Clinical Cardiac Electrophysiology: Techniques and Interpretation*, 2nd ed. (Lea Fabiger, Philadelphia, 1993); *From Cell to Bedsize: Cardiac Electrophysiology*, edited by D. P. Zipes and J. Jalife (W.B. Saunders, Philadelphia, 1995).

[15] W. Jahnke and A. T. Winfree, Int. J. Bifurcation Chaos Appl. Sci. Eng. **1**, 445 (1991).

[16] H.-J. Krug, L. Pohlmann, and L. Kuhnert, J. Phys. Chem. **94**, 4862 (1990).

[17] M. Gómez-Gesteira, A. P. Muñuzuri, V. Pérez-Muñuzuri, and V. Pérez-Villar, Phys. Rev. E **53**, 5480 (1996).

[18] M. Ruiz-Villarreal, M. Gómez-Gesteira, C. Souto, A. P. Muñuzuri, and V. Pérez-Villar, Phys. Rev. E **54**, 2999 (1996).

[19] M. Ruiz-Villarreal, M. Gómez-Gesteira, and V. Pérez-Villar, Phys. Rev. Lett. **78**, 779 (1997).

[20] A. S. Mikhailov, *Foundations of Synergetics I* (Springer-Verlag, Berlin, 1995).

[21] A. S. Mikhailov, V. A. Davydov, and V. S. Zykov, Physica D **70**, 1 (1994); Sov. Phys. Usp. **34**, 665 (1991).